



Nano-structural changes in SiO₂ amended clay concrete under Alkali silica treatment

N. Tahiri^{1,2*}, L. Khouchaf¹, M. Elaatmani², A. Zegzouti², M. Daoud²

¹IMT Lille Douai, Université de Lille, Research Center of Ecole des Mines de Douai, Rue Charles Bourseul CS10838, 59808, Douai, France.

²Cadi Ayyad University, Department of chemistry, Faculty of Sciences Semlalia, Bd Prince My Abdellah, 40000, Marrakech, Morocco.

Received 07 Jun 2017,
Revised 03 Aug 2017,
Accepted 12 Aug 2017

Keywords

- ✓ Alkali-silica reaction,
- ✓ Aggregate,
- ✓ Concrete,
- ✓ Bentonite,
- ✓ Durability,

nabiha.tahiri@ced.uca.ac.ma;
Phone: +212616490311;

Abstract

In this study, the structural changes of natural SiO₂ aggregate at the nanometric scale during the attack by the alkali-silica reaction (ASR) are followed. The effect of the bentonite as a partial substitution of the cement in concrete is investigated. The samples are analyzed by X-ray diffraction (XRD), Infrared spectroscopy (IR), transmission electronic microscopy (TEM) and Energy Dispersive Spectrometer (EDX). The structural changes that occur in the aggregate at different times of ASR were well highlighted at the nanometric scale. The X-ray diffraction and infrared spectroscopy analysis showed that the reactivity of the aggregate decreases with the presence of the bentonite. This result allowed us to conclude that partial substitution of the bentonite in the concrete is effective against expansion by the ASR.

1. Introduction

The SiO₂ compounds are used as nano particles as strengthening additives in the potter's clay materials, as insulator in electronic and in glass industry or as aggregate in concrete. The latter is a composite material that consists essentially of a mixture of portland cement and water, within which are embedded particles of aggregate. Degradation of concrete widely depends on the crystalline quality of the aggregate. A chemical reaction is called the alkali-silica reaction (ASR) between the reactive silica SiO₂ aggregate and alkali content of the cement in the interstitial solution causes damages of concrete. Several research studies have been conducted to understand the chemical and mechanical mechanisms of this reaction and it is accepted that the mechanism of the reaction begins with the dissolution of the reactive silica contained in the aggregate under the action of OH⁻ ions in the pore solution followed by the migration of ionic species (K⁺, Na⁺ and Ca²⁺) to form Alkali Silica Reaction ASR gels [1, 2]. ASR gels are precipitated in the solid skeleton that induces swelling and microcracks into concrete [3, 4].

However, the existence of the ASR requires the presence of three factors: high alkali content in the interstitial phase of concrete, the presence of reagents in the aggregate and wet environment. Thus, in order to avoid the premature deterioration of the concrete by the ASR, we must eliminate one of these necessary factors. However, this is not always efficient and it is economically unsuitable. For this reason, another preventing method which is more economical and compliant is used such as heat treatment of natural aggregate to improve its crystallinity [5], use chemical admixtures like lithium salts [6] or complementary cementing materials like fly ash [7], silica fume [8], glass powder [9], groud clay brick [10], kaolinite [11] ... In the present research, our approach is to use the bentonite as a partial cement replacement. The use of bentonite could reduce energy consumption, solve environmental problems related to cement production and improve the durability of the concrete structures.

Bentonite is highly colloidal clay. It is mainly composed of montmorillonite which is a clay mineral of the smectite group. It is in the form of sheets; each sheet consists of three layers, a core layer of Al octahedral and two tetrahedral layers of Si. Water molecules are inserted between the layers. The substitution of Al³⁺ by

lower valence ions Mg^{2+} et Fe^{2+} / Fe^{3+} , and the partial substitution of Si^{4+} by Al^{3+} makes the structure not electrically neutral which explains the presence of cations Ca^{2+} , Na^+ , K^+ , Mg^{2+} ... which are adsorbed between the layers to neutralize the negative charge [12].

The choice of the amount of cement replaced by bentonite is important to keep concrete proprieties. Miriza [13], mentioned in their work that the substitution of cement with an amount of bentonite which is above 30% causes the decrease of the workability of concrete and its compressive strength. According to Shazim [14], the substitution of the cement with an amount of bentonite which is less than 21% leads to an increase of the compressive strength.

This research study is devoted to showing the ASR effect on the flint (aggregate) structure at the nanometer scale, and to evaluate the influence of bentonite within the concrete to limit ASR expansion through the study of the flint structure.

2. Material and Methods

2.1. Samples preparation

Two types of samples have been prepared; samples with and without partial substitution with bentonite. The preparation protocol of samples without substitution and with bentonite is as follows: 0.5 g of crushed flint was placed in the autoclave and then 0.1892g of calcium oxide (CaO) was added to simulate the cement matrix. 5ml of potash solution KOH (0.79 mol/l) to simulate the interstitial solution of the concrete [15, 16]. Samples with partial substitution with bentonite have been prepared in the same way as the first type of samples except that 20% of CaO was substituted by bentonite.

To accelerate the reaction, the autoclave was put in an oven at 80°C during 312h.

To follow the evolution of silanols after the chemical attack into these samples, other samples T_4 -312- e_2 and T_4 -bent-312- e_2 have been prepared. This type of sample is obtained after a chemical treatment with hydrochloric acid of samples T_4 -312- e_1 and T_4 -bent-312- e_1 in order to remove all cations and keep only the undissolved silica [17]. The samples descriptions are summarized in table 1.

Table 1: Samples descriptions.

Sample	Description
T_4	raw flint
T_4 -30- e_1	sample contains reaction products and raw flint attacked by ASR for 30h
T_4 -312- e_1	sample contains reaction products and raw flint attacked by ASR for 312h
T_4 -bent-312- e_1	sample contains reaction products and raw flint attacked by ASR for 312h in presence of bentonite
T_4 -312- e_2	sample contains only raw flint attacked by ASR for 312h
T_4 -bent-312- e_2	sample contains only raw flint attacked by ASR for 312h in presence of bentonite

2.2. Characterization

2.2.1. Transmission electron microscopy (TEM)

The TEM investigations were performed with a FEI Tecnai G2-20 instrument operating at 200 kV accelerating potential. It is equipped with a filament of lanthanum hexaboride LaB_6 , a double-tilt holder and Gatan digital camera.

2.2.2. X-ray diffraction (XRD)

X-ray powder data were collected in the reflection mode using a Shimadzu Bruker D8 Advance diffractometer (Cu-K λ radiation = 1.5418 Å). The measurements were performed with a step length of 0.02° in the range of 5°-100° at the scanning speed of 0.5 s/step. Accelerating voltage and electric current were 40 kV and 40 mA, respectively

2.2.3. Infrared spectroscopy (IR)

Infrared data were obtained by the transmittance method on a Perkin Elmer spectrometer. The samples therefore were diluted by KBr (about 1 mg sample in 99 mg KBr), pressed into pellets and measured relatively to the KBr as a reference.

3. Results and Discussion

3.1. Structural modification of the aggregate during the ASR

The development of an ASR model at the microscopic level has a major role to the understanding of the mechanisms involved in the ASR. Electron microscopy is well suited to observe materials with scales ranging from nanometer to micrometer. It provides access to their microtexture and their microstructure.

Figure 1 shows TEM image of the aggregate T_4 before the reaction process. From this image, we can observe zones with well-defined geometrical grains and angular sides of 120° characterizing angles of crystalline silica. The grains have different sizes ranging from ten nanometers to a few hundred micrometers. Moreover, zones without defined form are observed and may be attributed to the amorphous fraction. From this image, we can deduce that the starting aggregate is heterogeneous and contains structural defects.

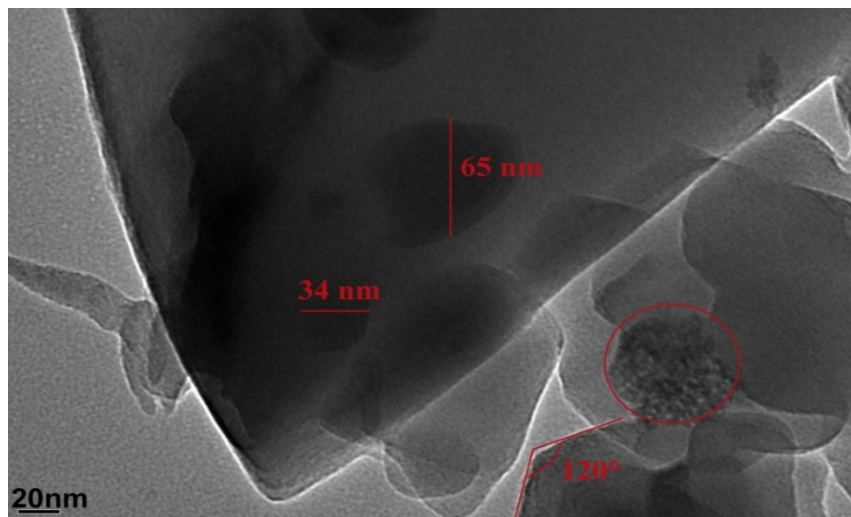


Figure 1: TEM micrographs of T_4

The TEM micrograph of T_4 -30- e_1 sample is shown in figure 2. The image shows the heterogeneity of the attack. Zone 1 resists to the reaction because it still presents the hexagonal angles attributed to the ordered SiO_2 phase. Zone 2 shows a fibrillar and layered morphology; the presence of this structure is associated to the formation of the phase of calcium silicate hydrates CSH [18]. This implies that zone 2 is more attacked by the ASR reaction.

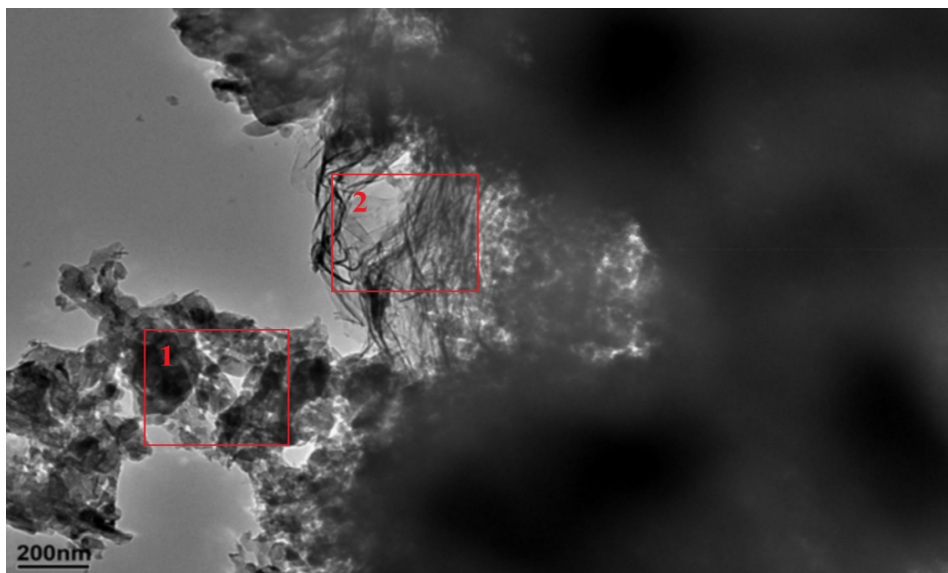


Figure 2: TEM micrograph of T_4 -30- e_1

In the figure 3 are shown the microanalysis spectra corresponding to the zones (1) and (2) of the figure 2. The nano-analysis corresponds with the observations made in figure 3. The EDX spectrum of the zone (1) shows that silicon and oxygen are the main components of this region while they are present in low proportions of calcium and potassium. The EDX spectrum of the zone (2) of the same figure shows the presence of intense peaks of silicon and oxygen. Moreover, it presents peaks calcium and potassium whose intensity has become greater compared to those of zone (1). In addition, carbon and copper are attributed to the grid of existing elements.

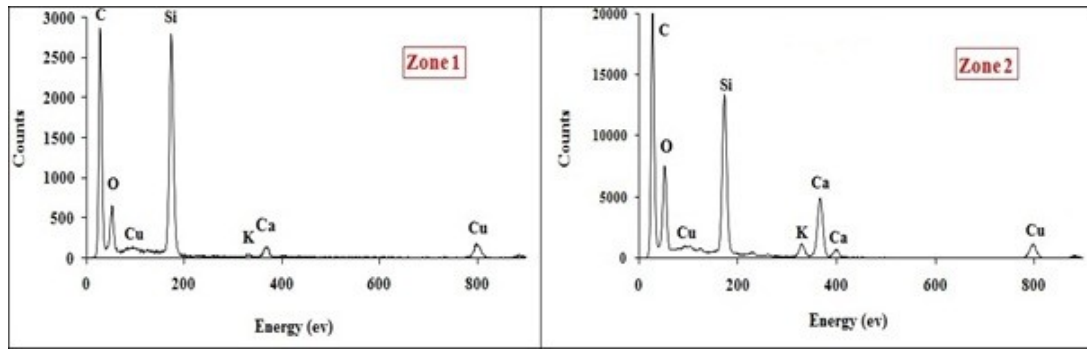


Figure 3: EDX analysis of the zones (1) and (2) of the figure 2

Furthermore, it is also noted that figure 4 shows the TEM micrograph of the sample T₄-312-e₁ where the EDX spectrum of the selected zone reveals essentially calcium, silicon, oxygen and potassium.

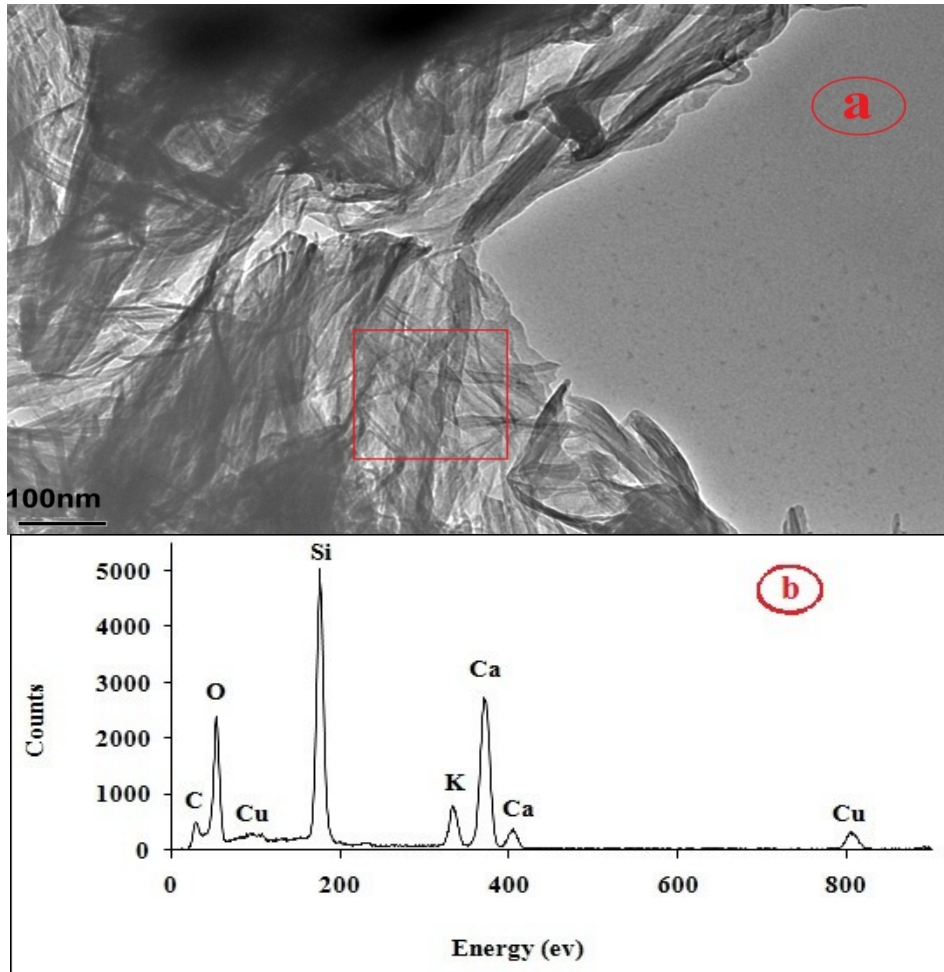


Figure 4: (a) TEM micrograph of T₄-312-e₁ and (b) EDX analysis of selected zone

Based on transmission electron microscopy combined with EDX analysis, it is showed that the structural and chemical changes that occur during the progress of the ASR at nanometric scale could be followed. TEM observations show that the aggregate has a heterogeneous structure which makes it sensitive to the effects of the ASR. When the aggregate is submitted under the ASR attack during 30h, it is clear that the reaction products begin to appear, which means that poorly crystallized zones are in the process of dissociating. After an ASR attack during 312h of the aggregate, only the laminated structure characterizing the CSH phases is observed; this means that the reaction reached a very advanced state.

3.2. Effect of partial substitution of bentonite

As mentioned above, the feasibility of bentonite in the concrete through the study of the flint structure was evaluated. In fact, the more the flint structure is dissociated, the more the reaction is advanced.

Figure 5 shows the XRD patterns of the T₄-312-e₁ and T₄-bent-312-e₁ samples. For both samples, the presence of peaks attributed to quartz and others corresponding to CSH phases is noticed.

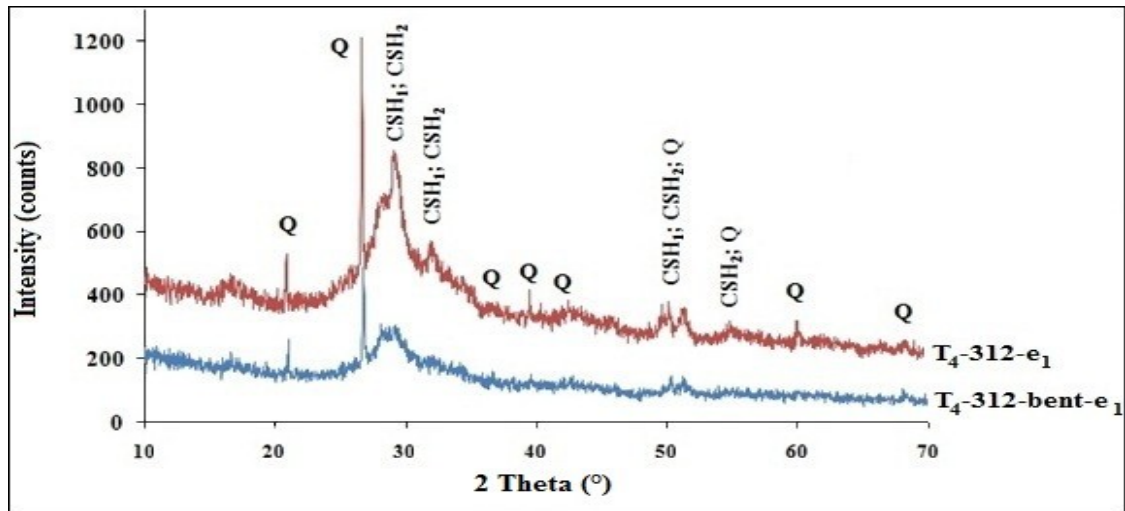


Figure 5: XRD patterns of T₄-312-e₁ and T₄-bent-312-e₁[CSH₁:Ca_{16.5}H_{22.22}O₅₀Si_{11.11} (PDF: 00-033-0306); CSH₂:Ca_{12.5}H₂₅O₅₀Si_{12.5} (PDF: 00-006-0013)]

Based on the XRD patterns, the Full Width at Half Maximum (FWHM) corresponding of the peak (101)-SiO₂ of samples T₄-312-e₁ and T₄-bent-312-e₁ is used to follow the relationship between the reactivity of SiO₂ aggregate and the bentonite substitution. Figure 6 shows the FWHM evolution of the diffraction peak (101)-SiO₂ of T₄ after 312h of the attack by the ASR (T₄-312-e₁ and T₄-bent-312-e₁). Compared to starting T₄, the FWHM of the T₄-312-e₁ sample represents 50% whereas the FWHM of the T₄-bent-312-e₁ sample represents 69%. In fact, poorly crystalline zones contribute to FWHM of the diffraction peaks.

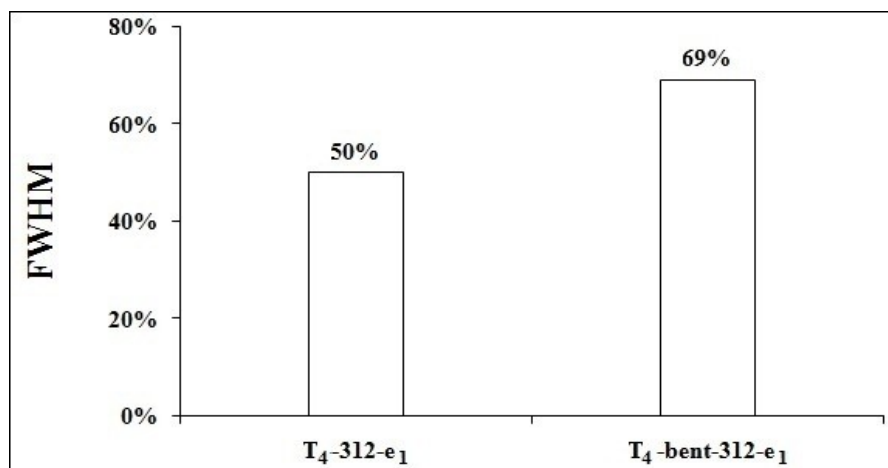


Figure 6: FWHM evolution of the diffraction peak (101)-SiO₂ of T₄-312-e₁ and T₄-bent-312-e₁

Initially, the attack by the ASR causes the destruction of zones containing structural defects [19, 20]. When these zones are altered by the reaction, it appears that the crystallographic structure of flint shows a decrease of its disorder. Therefore, the FWHM peaks decreases. This decrease may be explained by the appearance of zones with high crystallinity degree. This means that the aggregate in absence of bentonite is more attacked by the ASR than the aggregate with the presence of bentonite. In fact, bentonite dissociation is carried out using the OH⁻, and the pozzolanic reaction consumes Ca(OH)₂, which induce a decrease of the Ca²⁺ and OH⁻ concentration. In addition, it is well known that both Ca(OH)₂ and high OH⁻ ions concentration are necessary for concrete expansion by ASR [21, 22]. This may explain why T₄ in absence of bentonite is more dissociated and attacked by the ASR than T₄ in his presence.

Following the evolution of bands characterizing the silanols vibration located at 555 cm⁻¹ and 950 cm⁻¹ [23, 24], may be also an indicator to determine the reactivity of T₄ against ASR in presence and absence of bentonite. In fact, the intensities of these bands increase with the increasing reaction time. This means that when siliceous aggregate is attacked, the intensities of these bands increase. From figure 7, the intensities of the 555 cm⁻¹ and 950 cm⁻¹ bands are more intense for T₄-312-e₂ than T₄-bent-312-e₂. This means that there is more creation of Si-OH in T₄-312-e₂ than in T₄-bent-312-e₂. This result shows that T₄ is less attacked by the ASR in the presence of bentonite in agreement with the result of FWHM evolution of the T₄-312-e₁ and T₄-bent-312-e₁ samples. This is an explanation of the role played by the bentonite to limit ASR progress.

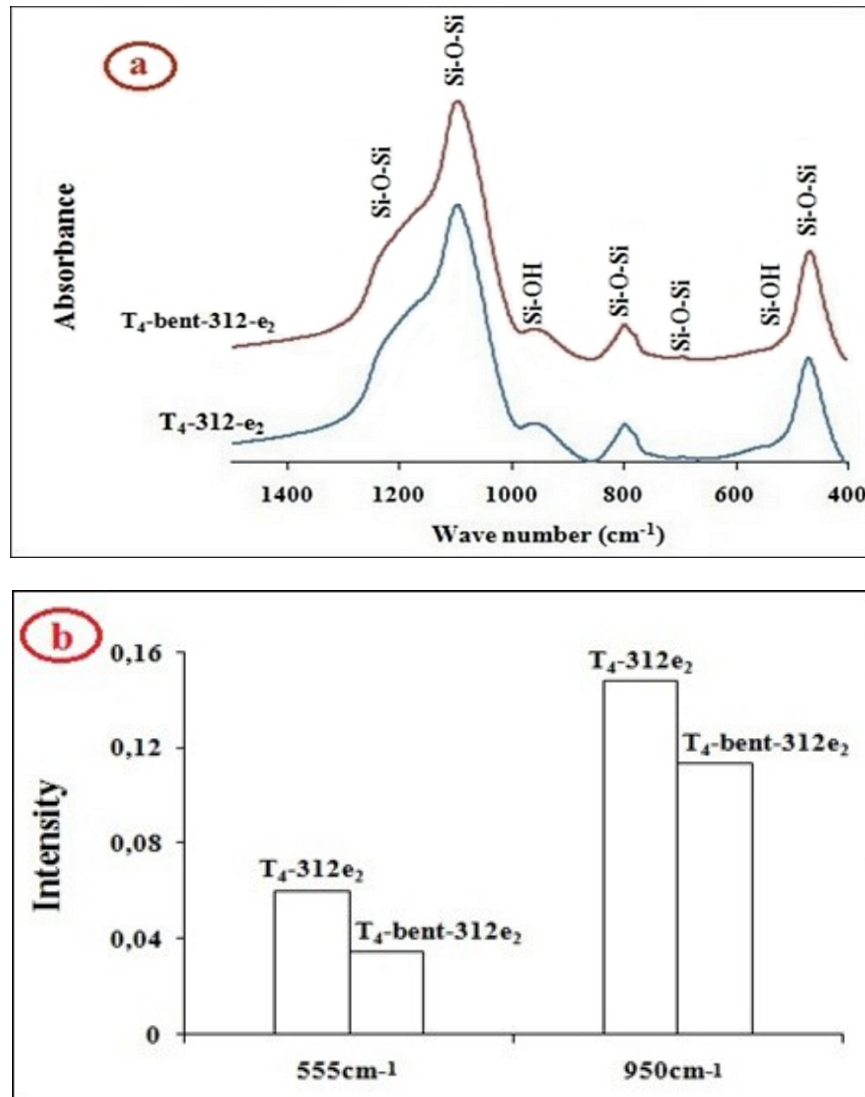


Figure 7: a- Infrared spectra of T_4 -312- e_2 and T_4 -bent-312- e_2
 b- Intensity of 555cm^{-1} and 950cm^{-1} bands of T_4 -312- e_2 and T_4 -bent-312- e_2

Conclusion

In this paper, the structural changes of SiO_2 natural aggregate during the attack by ASR at the nanometric scale are followed. In addition, the effect of partial substitution of bentonite is highlighted.

Thanks to TEM and EDX microanalysis, the transformation of the SiO_2 aggregate to CSH under ASR reaction at the nanometer scale is shown. Following the evolution XRD patterns and the intensity of infrared bands at 555cm^{-1} and 950cm^{-1} showed the benefit of the partial substitution of bentonite to limit the ASR progress. In fact, in the presence of bentonite, the ions of Ca^{2+} and OH^- will be consumed by dissociation of this material, on the one hand and, on the other, the interaction of bentonite with these ions leads to the formation of pozzolanic CSH which have the property of absorbing a large quantity of alkali ions, thus causing the reduction of the alkalinity of the interstitial solution of the concrete.

In fact, the use of bentonite within the concrete can provide one of the best solutions to decrease the expansion due to alkali silica reaction through the protection of the concrete skeleton and provide a positive impact on the durability of the concrete.

References

1. L. Khouchaf, J. Verstraete, *J. Mater. Sci.* 42 (2007) 2455–2462.
2. F. Boinski, L. Khouchaf, M.H. Tuilier, *J. Mater. Chem. Phys.* 122 (2010) 311–315.
3. P. Rivard, J.P. Ollivier, G. Ballivy, *J. Cem. Concr. Res.* 32 (2002) 1259 – 1267.
4. V. E. Saouma, R.A. Martin, M.A. Hariri-ardebili, T. Katayama, *J. Cem. Concr. Res.* 68 (2015) 184-195.

5. N. Tahiri, L. Khouchaf, M. Elaatmani, G. Louarn, A. Zegzouti, M. Daoud, *IOP Conference Series: Mater. Sci. Eng.* 62 (2014) 012002, doi:10.1088/1757-899X/62/1/01200200.
6. T. Kim, J. Olek, *J. Cem. Concr. Res.* 79 (2016) 159–168.
7. F. B. Roland, D.A.T. Michael, *J. Adv. Cement Based Mater.* 7 (1998) 66–78.
8. J. Duchesne, M. A. Bérubé, *J. Cem. Concr. Res.* 24 (1994) 73–82.
9. A. Shayan, A. Xu, *J. Cem. Concr. Res.* 34 (2004) 81–89.
10. L. Turanli, F. Bektas, P. J. M. Monteiro, *J. Cem. Concr. Res.* 33 (2003) 1539–1542.
11. R. Fernandez, F. Martirena, K. L. Scrivener, *J. Cem. Concr. Res.* 41 (2011) 113–122.
12. B. Tyagi, C.D. Chudasama, R. V. Jasra, *J. Spectrochim. Acta, Part A.* 64 (2006) 273–278.
13. J. Mirza, M. Riaz, A. Naseer, F. Rehman, A. N. Khan, *J. Appl. Clay Sci.* 45 (2009) 220–226.
14. A. S. Shazim, R. Arsalan, S. Khan, T. Yiu, *J. Constr. Build. Mater.* 30 (2012) 237–242.
15. F. Boinski, L. Khouchaf, J. Verstraete, M. H. Tuilier, *J. Physic. IV.* 118 (2004) 277–281.
16. J. Verstraete, L. Khouchaf, *J. Mater. Sci.* 39 (2004) 6221–6226.
17. J. Verstraete, L. Khouchaf, D. Bulteel, E. Garcia-diaz, A. M. Flank, M. H. Tuilier, *J. Cem. Concr. Res.* 34 (2004) 581–586.
18. F. Pelisser, P. J. P. Gleize, A. Mikowski, *J. Cem. Concr. Compos.* 48 (2014) 1–8.
19. L. Khouchaf, J. Verstraete, R.J. Prado, M. H. Tuilier, *J. Phys. Scripta.* T115 (2005) 552–555.
20. I. G. Richardson, *J. Cem. Concr. Res.* 38 (2008) 137–158.
21. L. Struble, S. Diamond, *J. Cem. Concr. Res.* 11 (1981) 611–617.
22. S. Chatterji, *J. Cem. Concr. Res.* 9 (1979) 185–188.
23. M. Domanski, J. A. Webb, *J. Archaeol. Sci.* 19 (1992) 601–614.
24. C. W. B. Burnham, J. R. Holloway, N. F. Davis, *Geol. Soc. Am.* 132 (1969) 1–96. doi:10.1130/SPE132-p1.

(2018) ; <http://www.jmaterenvirosci.com>